Semi-Annual Report Submitted to the
National Aeronautics and Space Administration

For January - June, 1992

Contract Number: NAS5-31370

Land Surface Temperature Measurements from EOS MODIS Data

MODIS Team Member
PRINCIPAL INVESTIGATOR

ZHENGMING WAN
Center for Remote Sensing and Environmental Optics
University of California, Santa Barbara

P.I.'s Address:

ZHENGMING WAN
Computer Systems Laboratory, Girvetz 1140
Center for Remote Sensing and Environmental Optics
University of California
Santa Barbara, CA 93106-3060

phone : (805) 893-4541
Fax no: (805) 893-2578
Internet: wan@crseo.ucsb.edu

Land Surface Temperature Measurements from EOS MODIS Data

Semi-Annual Report
For January - June, 1992

Zhengming Wan, University of California at Santa Barbara
Contract Number: NAS5-31370

1. Task Objectives

Based on current conditions that an IBM workstation RISC/6000 320H was purchased by the end of the last year, that spectral emissivities of land covers are still very limited in open literatures, and that there is no instrument for the principle investigator to make spectral emissivity measurements, the following task objectives were set for this year:

1) to port the atmospheric radiative transfer code ATRAD to the IBM workstation from a SUN workstation, and to improve its performance;

2) to make an in-depth investigation of the effect of temperature-dependent molecular absorption;

3) to verify reasonable requirements for the accuracy of radiative transfer models to be used for development of land-surface temperature (LST) algorithms and requirements for MODIS specifications based on analysis of the existing validated multi-channel sea-surface temperature algorithm for NOAA AVHRR data;

4) to develop an accurate radiative transfer model which will be suitable for development of LST algorithms.

2. Work Accomplished

2.1. ATRAD Has Been Ported to the IBM Workstation

The atmospheric radiative transfer code ATRAD and related programs have been ported to the new purchased computer IBM RISC/6000 320H from a SUN workstation. A few small modifications have been made according to the IBM AIXV3 conventions. A major effort was made to improve the speed of ATRAD by taking the advantage of bigger main memory in the IBM workstation. In the original version of my ATRAD code, a disk space is used to store the intermediate results which will be retrieved for quick calculations in consequent multiple boundary conditions (for different values of surface temperature and emissivity). After modification, a space of 26 Mb in main memory could be used as a primary space for storage and retrieval of the intermediate results. A disk space will be also used if more space is required. Using main memory as the primary storage space results in a significant improvement of performance. For a typical run which contains 10 different boundary conditions, the new computer time is about 50% of the original time in case of using disk space. The overall performance of ATRAD on the IBM workstation is about 10 times faster than the performance on SUN 3/60 used before. This has provided a much better condition for making multiple scattering radiative transfer simulations at a higher spectral resolution and with more molecular absorption terms.

2.2. Investigation of the Effect of Temperature-Dependent Molecular Absorption

2.2.1. Necessity

In order to better understand the entire Earth system on the global scale, the Earth Observing System (EOS) will provide surface kinetic temperatures of oceans and land, at specified accuracies of 0.2 K and 1 K in the 270-340 K range, respectively [1]. The international Tropical Ocean Global Atmosphere (TOGA) program has specified the sea surface temperature (SST) accuracy of 0.3 K as a requirement for global numerical models of climate. Compared to the accuracy of about 0.7 K achieved by the AVHRR instruments on the NOAA satellites [2, 3], the EOS's specified accuracies for SST and LST represent great challenges in the sensor design and algorithm developments. In the later respect, the major difficulty is in accurate corrections of atmospheric effects in satellite measurements of the surface temperature. The wide used multi-channel SST (MCSST) algorithm takes the form of a simple linear combination of the temperatures measured in different channels. Minnett [4] analyzed advantages and disadvantages of two approaches to determine the coefficients in MCSST: the empirical method

and the simulation method. Because of few in-situ LST data available and the inherent difficulties in ground-based LST measurements: surface heterogeneity, structure and shadowing, the LST algorithm will mainly depend on the simulation method. It requires that radiative transfer simulations produce very accurate radiance values to be measured by satellite sensors in the whole involved thermal infrared region in order to achieve the specified LST accuracy. However, experience indicates that most radiative transfer simulations, even those that are based on temperature and humidity profiles from balloon borne radiosonde, could not match the sea surface band brightness temperatures from satellite AVHRR data and the ship-based radiometric SST measurements within 0.3K, for example, as shown in Marton's recent study [5]. Besides errors due to various approximations in thermal infrared radiative transfer simulations, one important reason is the uncertainties in the temperature-dependent molecular absorption coefficients. The absolute accuracy of the measured Lorentz broadening coefficients of water vapor may range from ~ 4% for strong lines to ~ 30% for weak lines [6]. The temperature dependence of water vapor absorption coefficients does not seem to have been measured well for temperature below 20 °C [7]. Therefore, it is necessary to investigate the effects of different molecular absorption models and different approximations used in some wide used atmospheric radiative transfer models on surface temperature measurements.

2.2.2. Atmospheric Radiative Transfer Models

We have compared results from following atmospheric radiative transfer models.

LOWTRAN 6 — The last revised version of LOWTRAN 6 [8] was available since June 1983 and was wide used for atmospheric transmittance and radiance simulations. Numerical tables at spectral interval 5 cm^{-1} are used for temperature-independent band model absorption coefficients C_i, i = 1 for water vapor, 2 for CO_2+, i.e., uniformly mixed gasses including CO_2, HO_2, CO and CH_4, and 3 for infrared ozone. The transmission function is expressed as

$$\tau_i = \exp\{-C_i W_i\}\ ,\quad W_i = (\frac{P}{P_0})^{2n_i}(\frac{T_0}{T})^{n_i} U_i\ . \tag{1}$$

where P is pressure, T, temperature, U_i, the molecular absorber amount, n_i, a single temperature scaling factor for each molecular. The water vapor continuum absorption was based on Burch's earlier measurements [7]. The N_2 continuum absorption is considered in the 2080 to 2740 cm^{-1} region. The HNO_3 (nitric acid) absorption is considered in the 850-920, 1275-1350 and 1675-1735 cm^{-1} regions. The two-stream and single scattering approximations are used in LOWTRAN 6.

LOWTRAN 7 — We used the last revised version 4.2 of LOWTRAN 7 [9]. Numerical tables at spectral interval 5 cm^{-1} are used for temperature-independent band model absorption parameter C' (nominally sea level at 296 K) for eleven atmospheric molecules including H_2O, CO_2, O_3, N_2O, CO and CH_4, and O_2. The transmission function is expressed in the following double exponential form

$$\tau = \exp\{-(C W)^a\}\ ,\quad C = 10^{C'}\ ,\quad W = (\frac{P}{P_0})^m(\frac{T_0}{T})^n U\ . \tag{2}$$

where U is the molecular absorber amount, m, the pressure scaling factor, n, the temperature scaling factor. Different values of a, m, n are used for several broad wave number regions for each molecular. The new band models were developed with and based on degraded line-by-line spectra and validated against laboratory measurements. The water vapor continuum absorption was based on Burch and Alt's recent measurements [7]. A three-term K-distribution multiple scattering parameterization has been implemented in the LOWTRAN 7 model based on the two-stream approximation.

MODTRAN — It is a moderate resolution model of LOWTRAN 7 [10]. It has maintained all the LOWTRAN 7 options, i.e., aerosol models, standard atmospheric profiles or user-specified data. Band model parameters have been formulated from the HITRAN line atlas for twelve atmospheric molecules including H_2O, CO_2, O_3, N_2O, CO and CH_4, and O_2. They were calculated for 1 cm^{-1} bins from 0-17900 cm^{-1} and at five temperatures from 200 to 300 K. The transmission function is based on a statistical model for a finite number of lines within the spectral bin, and is given by

$$\tau = (1 - \langle W_{sl} \rangle)^{\langle n \rangle}\ . \tag{3}$$

where $\langle W_{sl} \rangle$ is the Voigt single line equivalent width for the line strength distribution in the spectral bin, $\langle n \rangle$,

the path averaged effective number of lines in the bin and given by <1/d>, the path averaged line spacing [10]. Note that the Curtis-Godson approximation is used in the band transmission function calculation for a nonuniform path. The MODTRAN model is also based on the two-stream approximation but uses a multiple scattering approximation without K-distribution. The above transmission function approaches to the exponential form, i.e., Beer's Law only for a large <n>. But the MODTRAN model always uses the Beer's Law to calculate the optical depth of each layer from transmittance ratios. The optical depth is then used in radiance calculations.

ATRAD — The accurate multiple scattering radiative transfer model ATRAD used in our previous study [11, 12] has been modified and used in this study. The ATRAD model is based on the interaction principle and adding/doubling method, and validated with the discrete-ordinate method. The "exponential-sum-fitting" method [13] is used to calculate exponential-sums for each atmospheric molecular from LOWTRAN or MODTRAN transmission functions averaged over a given wave number interval for a series of absorber amount in a wide range. A same wave number interval of 5 cm^{-1} was used in exponential-sum-fitting for a better cross comparison. Then the Beer's Law can be used in multiple scattering radiative transfer for each term in the exponential-sum expansion. All cross terms in the product of exponential-sums for H_2O, CO_2+ and O_3 are included in calculations so that the overlap absorption is fully taken into consideration which is overlooked in most models such as LOWTRAN and MODTRAN. In order to accurately investigate the effect of temperature-dependent molecular absorption, separate exponential-sum tables are obtained for different temperature and pressure values in the wide ranges of 200 to 300 K and 1 to 1013.25 mb. The accuracy for each table is better than 0.3% for water vapor in the 8-13 μm region. Then the exponential-sum table at pressure 1013.25 mb and at temperature 296 K is used as a base table to find the best temperature and pressure scaling factors for each wave number interval by systematic search. It turns out that these two scaling factors not only vary with wavenumber but also weakly depend on temperature and pressure, respectively. The maximum error in using the base table combined with these temperature and pressure scaling factors to cover the wide temperature and pressure ranges is less than a few percents for water vapor band absorption. The error is usually larger for CO_2 because its line tail contribution to the band absorption is not a monotone increasing function of temperature in some spectral ranges. Therefore, we focus on the effect of H_2O temperature-dependent absorption first.

2.2.3. Simulation Results

Band Transmittance and Brightness Temperature — Because different molecular band models are used in LOWTRAN and MODTRAN codes, we will compare their results of transmittance and radiance as a first step. For simplicity, the "standard" tropical atmosphere is used with a rural aerosol distribution in the elevation range from 0 to 2 km, background tropospheric aerosol and stratospheric aerosol, and normal upper atmospheric aerosol in the upper ranges, the surface visibility at 0.55 μm being 23 km. The surface temperature is assumed to be equal to the surface air temperature 299.7 K. Because LOWTRAN and MODTRAN codes only support a simple form of surface refelctivity, i.e., albedo for a Lambertian grey-body surface, we use wavelength-independent albedo of 0.02 (so surface emissivity is 0.98) as a first order approximation of sea surface for all simulations except explicated otherwise. We will adopt the wavelength and angular dependent sea surface emissivity model into ATRAD simulations later. Suppose that MODIS and ASTER observe the earth surface at the nadir direction. In calculating band averaged transmittance and brightness temperature, the MODIS and ASTER spectral response function is simplified as follows: $\Psi(\lambda) = 1$ for $\lambda_{low} + 0.25\,\delta\lambda < \lambda < \lambda_{up} - 0.25\,\delta\lambda$; $\Psi(\lambda)$ linearly decreases to 0.5 at λ_{low} and λ_{up}; $\Psi(\lambda) = 0$ for $\lambda < \lambda_{low}$ and $\lambda > \lambda_{up}$, where $\delta\lambda = \lambda_{up} - \lambda_{low}$. But actual spectral response functions will be used for NOAA-7 AVHRR channels.

As shown in Table 1 where the second column is the band range, transmittance difference between MODTRAN and LOWTRAN7 in the third column could be as large as 6%, transmittance difference between MODTRAN and LOWTRAN6 in the fourth column is even larger because of the difference in water vapor continuum absorption, and band averaged brightness temperature differences in the last two columns can exceed 0.6 K. All these differences become larger as viewing zenith angle increases. For example, the transmittance could differ more than 30% near the edges of the thermal infrared atmospheric windows (3.4 - 4.1 and 8 - 13 μm) at a large viewing zenith angle. Because not only band absorption models but also detail methods used for radiative transfer solutions are different in LOWTRAN6, LOWTRAN7, and MODTRAN, it is difficult to identify which factors cause these differences.

TABLE 1. Comparison between MODTRAN and LOWTRAN in MODIS and ASTER thermal bands for a land surface at $T_s = T_{air} = 299.7$ °K and $\varepsilon = 0.98$ under tropical atmosphere with surface visibility 23 km at 0.55 μm and nadir viewing.

sensor band no.	band range (μm)	Δ(transmittance) $t_m - t_{l7}$	$t_m - t_{l6}$	$T_{mod} - T_{low7}$ (°K)	$T_{mod} - T_{low6}$ (°K)
MODIS					
20	3.660-3.840	+6.0%	-2.1%	0.77	0.48
22	3.934-3.984	+1.9%	-1.3%	0.29	0.44
23	4.025-4.075	+3.7%	-2.0%	0.55	0.29
29	8.400-8.700	-0.7%	+1.2%	0.32	0.62
31	10.78-11.28	-0.1%	+7.7%	0.21	1.23
32	11.77-12.27	+2.7%	10.9%	0.65	1.47
ASTER					
10	8.125-8.475	-2.7%	-1.6%	0.65	0.74
11	8.475-8.825	-0.4%	+0.8%	0.33	0.68
12	8.925-9.275	+1.3%	+9.8%	0.49	1.90
13	10.25-10.95	+1.0%	+9.6%	0.45	1.80
14	10.95-11.65	-0.6%	+6.8%	0.07	1.06

Cross Comparison and Factor Analysis — The wide used split-window MCSST algorithm [2], which was determined by regression analysis of many coincident satellite and drifting buoy measurements, is

$$T_{ss} = 1.0346 T_4 + 2.5779 (T_4 - T_5) - 10.05 \quad (4$$

where T_{ss} is sea surface temperature, T_4 and T_5 are brightness temperatures from NOAA-7 AVHRR data of the split channel 4 and channel 5 at 11 and 12 μm, respectively. They are all in degrees Kelvin. Another MCSST algorithm, the triple-window MCSST used in night time is

$$T_{ss3} = 1.0170 T_4 + 0.9694 (T_3 - T_5) - 3.42 \quad (5$$

where T_3 is the brightness temperature from NOAA-7 AVHRR channel 3 at 3.75 μm. The split-window MCSST has been used to evaluate the effect of different molecular absorption models and different approximations in radiative transfer on SST calculations.

Figure 1 shows the total transmittance of tropical atmosphere in the window 10-13 μm and its transmission functions for H_2O band and continuum and those for CO_2+ from MODTRAN, LOWTRAN7, and LOWTRAN6. It is found that the spectral features in MODTRAN's H_2O band transmittance is remarkable compared to those in LOWTRAN codes, and that MODTRAN and LOWTRAN6 have almost a same CO_2+ transmission function. Qualitative comparisons are given in Table 2. If there is a comma in the fourth to the last columns, the first part is the comparison of LOWTRAN6 or LOWTRAN7 to MODTRAN for the NOAA-7 AVHRR channel 4, the second part is for channel 5. ATRAD-LOW1 uses the H_2O exponential-sum table (EST) and O_3 EST that are based on model 4, i.e., LOWTRAN7, but the CO_2+ EST which is based on model 5 (LOWTRAN6). ATRAD-LOW2 uses all ESTs that are based on LOWTRAN7 for a close comparison with LOWTRAN7. ATRAD-MOD1 uses H_2O EST based on MODTRAN, CO_2+ EST based on LOWTRAN6, and O_3 EST based on LOWTRAN7. But ATRAD-MOD2 uses H_2O EST based on MODTRAN, CO_2+ EST and O_3 EST based on LOWTRAN7.

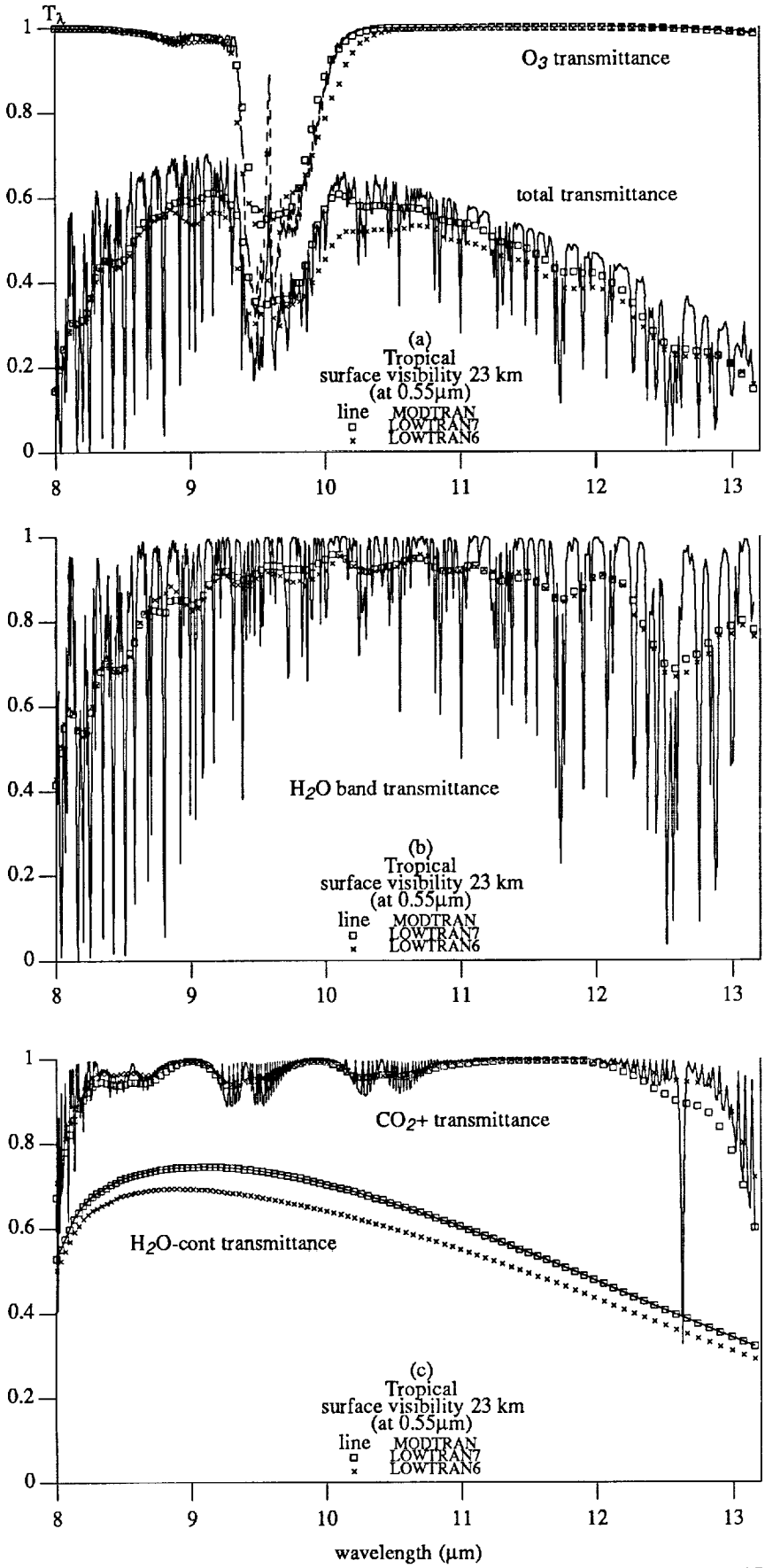

Figure 1. Comparison between transmission functions used in MODTRAN, LOWTRAN7, and LOWTRAN6.

TABLE 2. Comparison of molecular absorptions in different models with MODTRAN.

no.	model	spectral interval	H_2O-band	CO_2+	O_3	H2O-cont
1	MODTRAN	$1\,cm^{-1}$	model 1	model 1	model 1	=model 4
2	ATRAD-MOD1	$5\,cm^{-1}$	≈model 1	≈model 5	≈model 4	=model 4
2'	ATRAD-MOD2	$5\,cm^{-1}$	≈model 1	≈model 4	≈model 4	=model 4
3	ATRAD-LOW1	$5\,cm^{-1}$	≈model 4	≈model 5	≈model 4	=model 4
3'	ATRAD-LOW2	$5\,cm^{-1}$	≈model 4	≈model 4	≈model 4	=model 4
4	LOWTRAN7	$5\,cm^{-1}$	+, −−	≈, +	≈, ≈	model 4
5	LOWTRAN6	$5\,cm^{-1}$	+, −	≈, +≈	+, ≈	++, +

Table 3 gives quantitative comparisons between different models in NOAA-7 AVHRR band brightness temperature and MCSST values simulated for the same tropical atmosphere with the boundary conditions mentioned above. Surface emissivity 0.98 is also used for simulation of sea surface. The viewing direction is at zenith angle 11.4 °. The last column is the difference between MCSST from the split-window algorithm and the input SST value of 299.7 K. MODTRAN overestimates SST by 0.87 K. But all LOWTRAN related models underestimate SST, LOWTRAN7 using the multiple scattering option underestimates SST by -0.52 K as indicated by case 4, LOWTRAN7-MS. LOWTRAN7-SS in case 4' means using the single scattering option. ATRAD-MOD1 and ATRAD-LOW2 give almost a same MCSST value lower than SST by 0.7 K but their band temperatures are quite different (ΔT_4 = 0.56 K, ΔT_5 = 0.79 K) because they use different H_2O and CO_2+ band absorption models. ATRAD-MOD2 gives the best result at a difference -0.33 K. If the marine aerosol model under a low wind speed 1 m/s instead of the rural aerosol is used in ATRAD-MOD1, MCSST value will increase by 0.05 K. Similarly, ATRAD-MOD2 would give its MCSST at a difference -0.28 K. Detail factor analyses are given in the second part of Table 3. The only difference between ATRAD-MOD2 and ATRAD-LOW2 is that the former uses H_2O EST based on MODTRAN but the later uses one based on LOWTRAN7. It shows that the effect of the difference in H_2O band absorption models on MCSST is about 0.39 K. In case 5' where the new H_2O continuum absorption model is adopted into LOWTRAN6, it makes MCSST to change by 0.52 K. Comparison between case 3' and case 3 shows the effect of the difference in CO_2+ band absorption. The multiple scattering makes a MCSST difference of 0.41 K as shown in the comparison of case 4' to case 4. If the multiple scattering approximation used in LOWTRAN7 is accurate enough, the difference between ATRAD-LOW2 and LOWTRAN7-MS comes from absorption overlap which is not considered in LOWTRAN7.

Comparison between ATRAD-MOD1 and MODTRAN is given in the last part of Table 3. The total difference in MCSST is up to 1.58 K. More detail comparison is not as simple as above comparisons because of many differences involved in these two models. If LOWTRAN7 does not use the K-distribution in the multiple scattering parameterization but use the same subroutine used in MODTRAN, it makes a small difference of 0.04 K in MCSST. And assume a same difference 0.20 K belongs to the absorption overlap. If bypassing the Curtis-Godson approximation used in MODTRAN, it results in a change of MCSST by -0.61 K. The remainder, 1.95 K, may belong to use of Beer's Law in MODTRAN and other factors including possible difference in CO_2+ absorptions. Although these factor analyses made for NOAA-7 AVHRR bands are not very definite, it is obvious that those approximations such as multiple scattering, using Beer's Law to calculate optical depths, the Curtis-Godson method, and omiting absorption overlap, are accurate in the 0.5-2% range for broad bands, and they all could make a significant difference in MCSST as far as the high requirement of SST accuracy is concerned. It is also obvious that variations in the molecular absorptions have critical effects on band brightness temperature and on SST and LST algorithms.

Comparisons in Different Atmospheric and Surface Conditions — Figure 2 shows the atmospheric effect on the band brightness temperature T_i defined as temperature deficit $T_s - T_i$ in different atmospheric and surface conditions. The surface air temperature T_{air} = 299.7 K for tropical atmosphere, 294.2 K for summer mid-latitude, and 257.2 K for winter sub-arctic. The earth surface temperature T_s is defined as $T_{air} + \Delta T_s$. ΔT_s = 0, 1.5, or 3.0 K, respectively for the tropical case. ΔT_s = 0, -2, or -4 K, respectively for the mid-latitude case. And ΔT_s = 0, 2, or 4 K, respectively for the sub-arctic case. The dashed lines indicate divisions between these three cases. Four pairs of band temperature deficit values at viewing zenith angles 11.4°, 26.1°, 40.3° and 53.7° has

TABLE 3. Quantitative comparisons between different models in NOAA7 AVHRR band brightness temperature and MCSST values simulated for tropical atmosphere, surface visibility 23 km at 0.55 μm, $T_{ss} = T_{air}$ = 299.7 °K, viewing at 11.4 °.

no.	MODEL	T_4 (°K)	T_5 (°K)	$T_4 - T_5$ (°K)	MCSST (°K)	MCSST − SST
1	MODTRAN	295.434	293.509	1.925	300.57	+0.87
2	ATRAD-MOD1	295.175	293.760	1.415	298.99	-0.71
2'	ATRAD-MOD2	295.117	293.531	1.586	299.37	-0.33
3	ATRAD-LOW1	294.674	293.207	1.467	298.60	-1.10
3'	ATRAD-LOW2	294.611	292.971	1.640	298.98	-0.72
4	LOWTRAN7-MS	294.872	293.261	1.611	299.18	-0.52
4'	LOWTRAN7-SS	294.441	292.814	1.627	298.77	-0.93
5	LOWTRAN6	293.641	292.422	1.219	296.89	-2.81
5'	LOWTRAN6	using H_2O-continuum in LOWTRAN7				
		293.993	292.714	1.279	297.41	-2.29

compare models	ΔT_4 (°K)	ΔT_5 (°K)	$\Delta(T_4 - T_5)$ (°K)	Δ MCSST (°K)	factors
2' - 3'	+0.51	+0.56	-0.05	+0.39	H_2O band difference
5' - 5	+0.35	+0.29	+0.06	+0.52	H_2O-cont difference
3' - 3	-0.06	-0.24	+0.17	+0.38	CO_2 band difference
4 - 4'	+0.43	+0.45	-0.02	+0.41	multiple scattering
3' - 4	-0.26	-0.29	+0.03	-0.20	overlap effect
1 - 2	+0.26	-0.25	+0.51	+1.58	following effects in model 1
	+0.02	+0.01	+0.01	+0.04	no k-distribution
	+0.26	+0.29	-0.03	+0.20	no overlap
	+0.13	+0.42	-0.29	-0.61	Curtis-Godson approx.
	-0.15	-0.97	+0.82	+1.95	Beer's law & others

been included in order to show the viewing angle effect. They are linked by a solid line for each ΔT_s for ATRAD-MOD2 results in tropical and mid-latitude cases. Although the results from ATRAD-MOD2 and LOWTRAN7 in tropical and mid-latitude cases almost lie on same lines, their band temperature deficits could differ by more than 0.2 K. In case of sub-arctic atmosphere, the values of the band temperature difference $T_4 - T_5$ in MODTRAN and ATRAD-MOD2 are significantly smaller than those in LOWTRAN7. And even in LOWTRAN7, $T_4 - T_5$ is only about one tenth of $T_s - T_4$ or $T_s - T_5$, which ranges from 1.34 to 2.18 K. This means that it is difficult to make accurate atmospheric correction by the split-window method for LST in cold and dry regions. At least one more channel is needed for accurate LST algorithms in this situation. We can recognize some regional dependence and angular dependence in this figure. For all these three models, the value of MCSST - SST decreases as the precipitable water content in the atmosphere decreases. Its absolute value increases with

viewing angle in ATRAD-MOD2 and LOWTRAN7 but decreases in MODTRAN. For example, in case of tropical atmosphere with ΔT_s = 0 K, MCSST - SST = -0.52, -0.62, -0.87 and -1.44 K, at these four viewing angles respectively, in LOWTRAN7. They are -0.33, -0.43, -0.66, and -1.18 K in ATRAD-MOD2, but are 0.87, 0.79, 0.57, 0.04 K in MODTRAN.

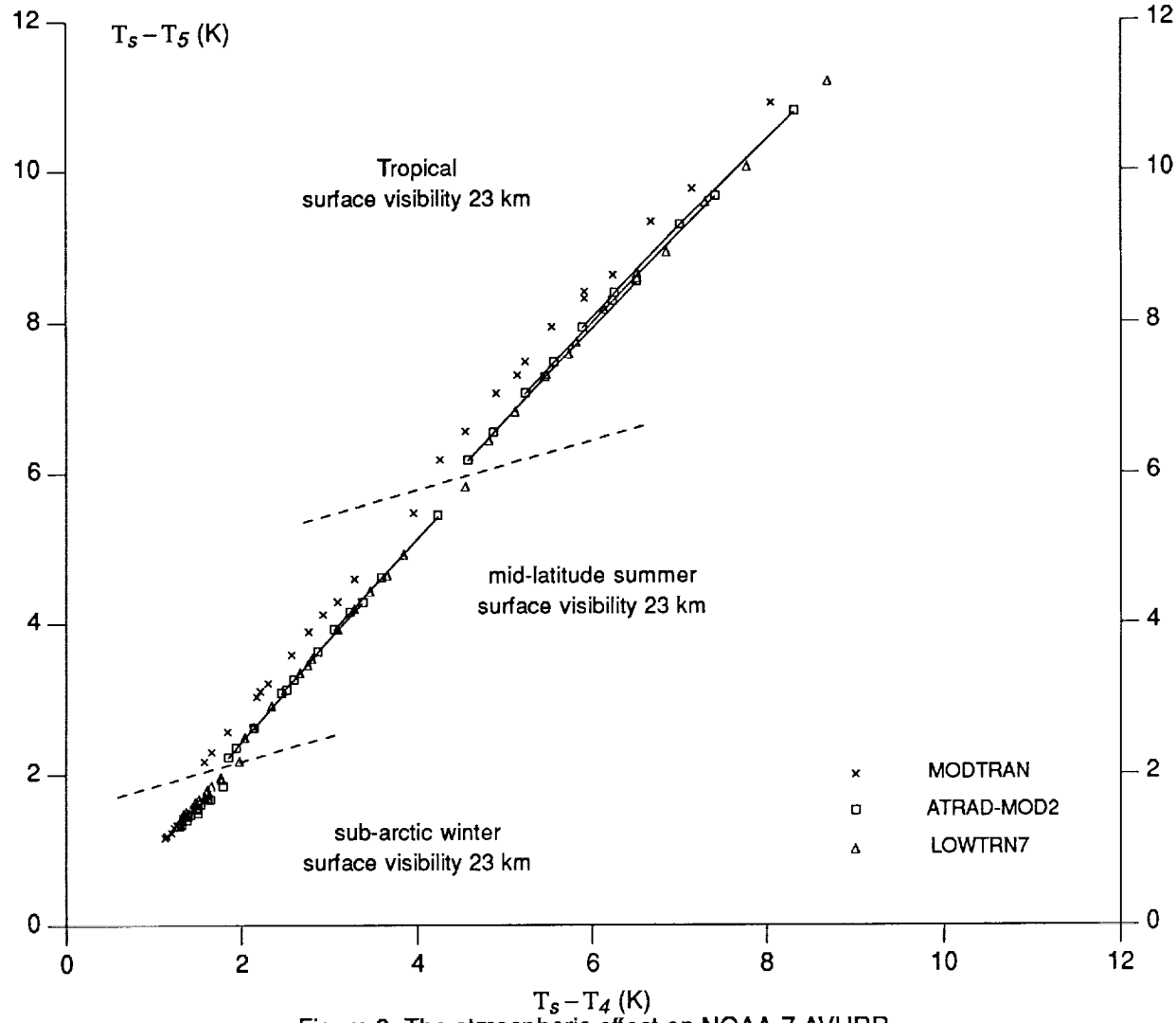

Figure 2. The atmospheric effect on NOAA-7 AVHRR band temperatures in different models.

Accuracy Requirements for Atmospheric Absorption Measurements We made some numerical experiments to see the effect of given variations in molecular absorption coefficients on the band brightness temperature. The summer mid-latitude atmosphere is taken as an example, assuming surface emissivity equal to 0.9. Results are shown in Table 4. In the second row, e H_2O-cont means that the exponential form of water vapor continuum absorption which is based on the dimer theory and recent measurements by Varansi [14] is used in ATRAD-MOD1. The variation of the water vapor self-broadening coefficient, C_s^0, with temperature follows the relation

$$\ln C_s^0 = \Theta / T + constant \, . \qquad (6$$

The value of Θ is 2501 K based on laboratory measurements and 2516 K based on the dimer theory. Changing water vapor continuum absorption model makes a difference 0.05 - 0.12 K for NOAA-7 AVHRR channel 4 and 0.09 - 0.18 K for channel 5. In the next row, +5% H_2O-bn means the water band absorption coefficient is increased by 5%. It makes band transmittances to decrease by 0.24% and 0.40% in channels 4 and 5, respectively. Its effect on band temperatures ranges from 0.01 to 0.04 K dependent on ΔT_s and viewing angle. The row indicated by -20% CO_2+ means the absorption coefficient of uniformly mixed gasses is decreased by

TABLE 4. Effects of Molecular Absorption Variations on NOAA-7 AVHRR Band Brightness Temperature.

MODEL	T_4 (°K) (11.4°)	(26.1°)	(40.3°)	(53.7°)	T_5 (°K) (11.4°)	(26.1°)	(40.3°)	(53.7°)
mid-latitude summer: T_s = 294.2°K, ε = 0.9								
ATRAD-MOD1	288.89	288.79	288.56	288.14	288.81	288.66	288.35	287.79
e H2O-cont	288.84	288.72	288.48	288.03	288.72	288.57	288.23	287.63
+5% H2O-bn	288.89	288.78	288.55	288.12	288.79	288.64	288.33	287.76
-20% CO2+	288.95	288.84	288.62	288.21	288.83	288.68	288.38	287.81
mid-latitude summer: T_s = 299.2°K, ε = 0.9								
ATRAD-MOD1	292.22	292.02	291.60	290.84	291.55	291.28	290.75	289.80
e H2O-cont	292.15	291.94	291.50	290.72	291.44	291.16	290.60	289.62
+5% H2O-bn	292.21	292.00	291.58	290.82	291.52	291.25	290.71	289.76
-20% CO2+	292.28	292.08	291.67	290.93	291.57	291.31	290.77	289.83

20%. It makes band temperatures to increase by 0.02 - 0.09 K. The CO_2+ absorption will make a larger effect in case of small precipitable water content. Therefore, the accuracy in molecular absorption measurements is needed at least better than 5% in order to develop accurate LST algorithms by the radiative transfer simulation method [15].

2.2.4. Sea-surface Emissivity Model

Taking the wavelength-dependence and angular dependence of sea-surface emissivity into consideration, the emissivity model of a calm sea surface [16] has been adopted into ATRAD, then model MCSST values change accordingly. In this sea surface emissivity model, the specular reflectance of sea surface is determined by Snell's Law and the wavelength-dependent refractive index of sea water [17, 18]. For a rough sea surface, its statistically averaged emissivity also depends on wind speed. Because wind speed data are usually not available, we only consider a calm sea surface here. In case of tropical atmosphere with $\Delta T_s = 0$K, ATRAD simulations give MCSST - SST = 0.34, 0.22, -0.10, and -0.87 K at four viewing angles 11.4, 26.1, 40.3 and 53.7 degree, respectively. As indicated in a review article by Robinson et al. [19], because of the effect of the sea surface thermal boundary layer, the surface skin of the ocean is typically 0.2 to 0.5 K lower than the bulk SST, which is the temperature recorded by ship or buoy measurements. And MCSST corresponds to the bulk SST, since it is based on regression analysis of coincident satellite and drifting buoy measurements. Therefore, the above values of MCSST - SST = 0.34 and 0.22 K at viewing angles 11.4° and 26.1° given by ATRAD is reasonable. However, according to Bates and Diaz [20], the mean MCSST standard deviations are always lower than in situ data (the bulk SST) from the comprehensive ocean-atmosphere data set (COADS), ranging from 0.03 to 0.45 K. After correcting this effect, MCSST - SST ranges from 0.79 to -0.42 K for viewing angle from nadir to 53.7°. This suggests that the viewing angle should be included into MCSST algorithms if satellite data at larger viewing angles still have enough sensitivity.

2.3. Requirements for Accuracy of Radiative Transfer Models and MODIS Specifications

Because the wide used McClain's split-window SST algorithm [2] is based on regression analysis of many coincident satellite and drifting buoy measurements, it could be used to determine requirements for the accuracy of radiative transfer models and for specifications of MODIS thermal bands. Under the assumption that NOAA7 AVHRR thermal channel data in Equations 4 and 5 have a same accuracy of band temperature, T_b, a simple error analysis of these two equations gives

$$\Delta T_{ss} = 6.19\,\Delta T_b \qquad (7$$

and

$$\Delta T_{ss3} = 2.96\,\Delta T_b\,. \qquad (7'$$

Equation 7 means that the specified SST accuracy of 0.3 K requires $\Delta T_b \leq 0.05$ K. In the wavelength range 10 to

13 μm, 1% of radiance change ($\Delta L / L$) at 300 K corresponds to a temperature change ΔT of about 0.7 K. So we can gain the following insights into the surface temperature problem:

1) A radiative transfer model with an accuracy at the 0.1% level is required in order to develop SST algorithms at the accuracy 0.3 K and LST algorithms at the accuracy 1 K [15];

2) For the MODIS thermal bands to be used for surface temperature measurements, the calibration accuracy is required better than 0.5% with a goal of 0.25%.

According to ATRAD simulations for a calm sea surface under the "standard" tropical atmospheric condition, as SST changes 0.25 K, the band brightness temperature at zenth angle 53.7° changes only 0.081 and 0.044 K in NOAA7 AVHRR channel 4 and 5, respectively. Because the radiometric resolution for AVHRR channels 4 and 5 using 10 bit numbers is around 0.1 K for typical SST between 270 and 300 K, and the noise equivalent difference temperature NEδT is around 0.12 K, AVHRR data are not sensitive enough to estimate SST at large viewing angles. Barton [5] has shown some examples of very poor agreements between MCSST and radiometric SST values at large viewing angles. Therefore, the MODIS specifications for 12 bit numbers and noise equivalent difference temperature NEδT at 0.05K are essential to achieve the high SST and LST accuracies for the whole swath of 2,300 km in which the instrument scans from $-55°$ to $+55°$.

It is very important to find some good ground validation sites for absolute calibration of the MODIS thermal bands. ATRAD simulations show that the atmospheric transmission function for summer midlatitude atmosphere over a lake surface at elevation 4 km above sea level is larger than 0.97 for the most part of the atmospheric window $10-13$ μm, and that the difference between the radiance at the top of the atmosphere and the radiance at the lake surface is less than 1% for the wavelength range from 10.4 to 12 μm. If a fair knowledge of atmospheric temperature and water vapor profiles is available, it seems not difficult to make an atmospheric correction to achieve the accuracy requirement of 0.2% for ground-based calibrations. The major uncertainty will be in measurements of the lake surface temperature. We need to make very accurate radiometric measurements. Or if we can find some alpine lakes which is partially frozen, then the temperature of the free water surface area is believed to be very close to zero degree C without measurements. Several such lakes are found in the Tibet region, but their sizes are only in the order of 10 by 10 km.

2.3.1. New Developments in the Radiative Transfer Model ATRAD

The wavelength-dependent and angular dependent emissivity model of pure water and sea water surfaces has been implemented in the radiative transfer model ATRAD. It could be used for development of accurate SST and lake surface temperature algorithms under the low wind speed condition. But uncertainties in surface reflectivity distributions make it difficult to achieve a high accuracy under high wind speed conditions.

3. Anticipated Future Actions

1) to continue on selection of ground validation sites and preparation of validation plan for MODIS thermal bands;

2) to make radiative transfer simulations under conditions of different zenith-dependent surface temperatures;

3) to make radiative transfer simulations under conditions of different assumed zenith-dependent surface emissivities;

4) to investigate the effect of assumed surface thermal BRDF on simulation results of MODIS thermal bands.

4. Problems

During the ISLSCP Americans Workshop on Remote Sensing of the Land Surface for Studies of Global Change, 23-26 June 1992, Columbia, Maryland, one common consciousness was very obvious that the land-surface temperature is a very important variable for studies of global change, but it is not possible to accurately measure from space in the next five years. The major difficulty is due to lack of knowledge of spectral surface emissivity and reflectivity of land covers. So it becomes very critical in the next a few years to gain this knowledge from ground spectroradiometric measurements in order to develop accurate LST algorithms before EOS launches.

5. Publications

Z. Wan and J. Dozier, Effects of temperature-dependent molecular absorption coefficients on the thermal infrared remote sensing of the earth surface, *Proceedings of 12th International Geoscience and Remote Sensing Symposium*, Houston, TX, May 26-29, 1992. pp. 1242-1245.

REFERENCES

[1] NASA, *EOS Reference Handbook*, 147 pp., Greenbelt, MD: NASA Goddard Space Flight Ctr., 1991.

[2] E. P. McClain, W. G. Pichel, and C. C. Walton, "Comparative performance of AVHRR-based multichannel sea surface temperatures," *J. Geophys. Res.*, vol. 90, no. C6, pp. 11587-11601, 1985.

[3] I. J. Barton, A. M. Zavody, D. M. O'Brien, D. R. Cutten, R. W. Saunders, and D. T. Llewellyn-Jones, "Thereotical algorithms for satellite-derived sea surface temperatures," *J. Geophys. Res.*, vol. 94, no. D3, pp. 3365-3375, 1989.

[4] P. J. Minnett, "The regional optimization of infrared measurements of sea surface temperature from space," *J. Geophys. Res.*, vol. 95, no. C8, pp. 13497-13510, 1990.

[5] I. J. Barton, "Infrared continuum water vapor absorption coefficients derived from satellite data," *Appl. Optics*, vol. 30, no. 21, pp. 2929-2934, 1991.

[6] C. P. Rinsland, A. Goldman, M. A. H. Smith, and V. M. Devi, "Measurements of Lorentz air-broadening coefficients and relative intensities in the $H_2{}^{16}O$ pure rotational and ν_2 bands from long horizontal path atmospheric spectra," *Appl. Optics*, vol. 30, no. 12, pp. 1427-1438, 1991.

[7] W. B. Grant, "Water vapor absorption coefficients in the 8-13-μm spectral region: a critical review," *Appl. Optics*, vol. 29, no. 4, pp. 451-462, 1990.

[8] F. X. Kneizys, E. P. Shettle, W. O. Gallery, J. H. Chetwynd, L. W. Abreu, J. E. A. Selby, S. A. Clough, and R. W. Fenn, "Atmospheric Transmittance/Radiance: Computer Code LOWTRAN 6," Rep. AFGL-TR-83-0187 (NTIS AD A137796), Bedford, MA: Air Force Geophys. Lab., 1983.

[9] F. X. Kneizys, E. P. Shettle, L. W. Abreu, J. H. Chetwynd, G. P. Anderson, W. O. Gallery, J. E. A. Selby, and S. A. Clough, "Users Guide to LOWTRAN 7," Rep. AFGL-TR-88-0177, Bedford, MA: Air Force Geophys. Lab., 1988.

[10] A. Berk, L. S. Bemstein, and D. C. Robertson, "MODTRAN: A moderate resolution model for LOWTRAN 7," Rep. GL-TR-89-0122, Burlington, MA: Spectral Sciences, Inc., 1989.

[11] Z. Wan and J. Dozier, "Land-surface temperature measurement from space: physical principles and inverse modeling," *IEEE Trans. Geosci. Remote Sens.*, vol. 27, no. 3, pp. 268-278, 1989.

[12] Z. Wan and J. Dozier, "Effects of the atmosphere and surface emissivity on the thermal infrared spectral signature measured from MODIS-N," in *Proceedings of 10th International Geoscience and Remote Sensing Symposium, Maryland, May 20-24, 1990*, pp. 189-192.

[13] W. J. Wiscombe and J. W. Evans, "Exponential-sum fitting of radiative transmission functions," *J. Comput. Phys.*, vol. 24, no. 4, pp. 416-444, 1977.

[14] P. Varanasi, "On the nature of the infrared spectrum of water vapor between 8 and 14 μm," *J. Quant. Spectros. Radiat. Transfer*, vol. 40, no. 3, pp. 169-175, 1988.

[15] Z. Wan and J. Dozier, "Effects of temperature-dependent molecular absorption coefficients on the thermal infrared remote sensing of the earth surface," in *Proceedings of 12th International Geoscience and Remote Sensing Symposium, Texas, May 26-29, 1992*, pp. 1242-1245.

[16] K. Masuda, T. Takashima, and Y. Yakayma, "Emissivity of pure and sea waters for the model sea surface in the infrared window regions," *Remote Sens. Environ.*, vol. 24, pp. 313-329, 1988.

[17] G. M. Hale and M. R. Querry, "Optical constants of water in the 200-nm to 200-μm wavelength region," *Appl. Optics*, vol. 12, no. 3, pp. 555-641, 1973.

[18] D. Friedman, "Infrared Characteristics of ocean water (1.5-15 μm)," *Appl. Optics*, vol. 8, no. 10, pp. 2073-2078, 1969.

[19] I. S. Robinson, N. C. Wells, and H. Charnock, "The sea surface thermal boundary layer and its relevance to the measurement of sea surface temperature by airborne and spaceborne radiometers," *Intl. J. Remote Sens.*, vol. 5, no. 1, pp. 19-45, 1984.

[20] J. J. Bates and H. F. Diaz, "Evaluation of multichannel sea surface temperature product quality for climate monitoring: 1982-1988," *J. Geophys. Res.*, vol. 96, no. C11, pp. 20613-20622, 1991.